

Use of two-photon polymerization for continuous gray-level encoding of diffractive optical elements

Baohua Jia and Jesper Serbin

Centre for Ultrahigh-bandwidth Devices for Optical Systems (CUDOS) and Centre for Micro-Photonics, Faculty of Engineering and Industrial Sciences, Swinburne University of Technology, Hawthorn, Victoria 3122, Australia

Hwi Kim and Byoung-ho Lee

School of Electrical Engineering, Seoul National University, Kwanak-Gu, Shinlim-Dong, Seoul 151-744, South Korea

Jiafang Li and Min Gu^{a)}

Centre for Ultrahigh-bandwidth Devices for Optical Systems (CUDOS) and Centre for Micro-Photonics, Faculty of Engineering and Industrial Sciences, Swinburne University of Technology, Hawthorn, Victoria 3122, Australia

(Received 20 October 2006; accepted 28 November 2006; published online 12 February 2007)

Generation of continuous gray levels in three-dimensional diffractive optical elements has remained a challenge with the current semiconductor microfabrication method. In this letter, the authors propose and demonstrate the use of the two-photon polymerization method for fabricating three-dimensional diffractive optical elements of continuous gray levels. This method is a mask-free and low-cost single-step process. It is shown that the multilevel-phase-encoded diffractive optical element fabricated in inorganic-organic hybrid polymer material facilitates the intensity distribution synthesis with a high diffraction efficiency approaching the theoretical limit. © 2007 American Institute of Physics. [DOI: 10.1063/1.2426923]

Diffractive optical elements (DOEs) refer to modulation devices for light field synthesis. With the great advanced computing resources, the analysis and synthesis of DOEs are performed in the framework of electromagnetics as well as relatively simple scalar optics.^{1,2} The important requirements for DOEs as a device include high transparency for high energy efficiency, fine vertical resolution for a continuous phase modulation dynamic range, and chemical as well as mechanical stabilities.

The formation of DOEs conventionally relies on semiconductor microfabrication technologies such as photolithography and deep dry etching,³ which offer high accuracy and reproducibility but require sophisticated techniques and a long process time and normally lack the flexibility to generate arbitrary structures to serve different applications. Although different fabrication approaches, such as employing high-energy-beam sensitive glass,⁴ using a direct e-beam or single-point laser writing,^{5,6} have been proposed so far, they involve a time-consuming chemical treatment and high cost. Their complicated retooling process is a factor hindering the rapid development of DOE devices. Furthermore, it is challenging to use these methods to fabricate a three-dimensional (3D) DOE for continuous gray-level encoding in intensity distribution synthesis because they do not have the flexibility to control the phase of each pixel individually.

Recently the two-photon polymerization (2PP) technique has been widely demonstrated as a powerful tool in the fabrication of high resolution 3D microstructures.⁷⁻¹¹ By tightly focusing femtosecond laser pulses into the volume of liquid polymer resin, 2PP can be triggered only in a tiny region around the focal spot, where the energy is higher than the

polymerization threshold. As a result, with the 2PP technique, it is possible to produce arbitrary 3D structures with subwavelength resolution in a single step.^{8,11} In this letter, we demonstrate the capability of the 2PP method for the fabrication of high quality 3D DOEs encoded with gray-level information through controlling the size and thickness of each polymerized pixel, thus leading to the possibility of the intensity distribution synthesis.

The principle of a DOE is based on the two-dimensional (2D) intensity distribution synthesis through the Fresnel diffraction,¹² as shown in Fig. 1. The optical field propagating between the DOE domain and the output plane is described by the Fresnel transform. The input field $\bar{G}(\Phi)$ that is a complex optical field on the DOE is represented by

$$\bar{G}(\Phi_{k,l}) = A \exp(j\Phi_{k,l}), \quad (1)$$

where A and $\Phi_{k,l}$ are the amplitude profile of the incident field and the phase modulation value at the (k,l) th relief pixel, respectively. Let the target diffraction image and the Fresnel transform be denoted by I and $\mathbf{Fr}(\cdot)$, respectively. The error function indicating the deviation between the diffraction image and the target image defined as

$$E(\Phi) = \sum_{m,n} \left| \sqrt{I_{m,n}} - |\mathbf{Fr}(A \exp(j\Phi))_{m,n}| \right|^2 / \sum_{m,n} |I_{m,n}|^2 \quad (2)$$

can be minimized by finding the optimal phase profile Φ with numerical optimization techniques. In this work the iterative Fourier transform algorithm (IFTA), which is the most popular algorithm for DOE design,^{13,14} was employed. In Fig. 1(b), one of the original 2D intensity distributions, which is a photo of the Sydney Opera House sampled by 128×128 points, is shown. Figure 1(c) presents the phase profile of this photo coded by the IFTA method. The DOE

^{a)} Author to whom correspondence should be addressed; electronic mail: mgu@swin.edu.au

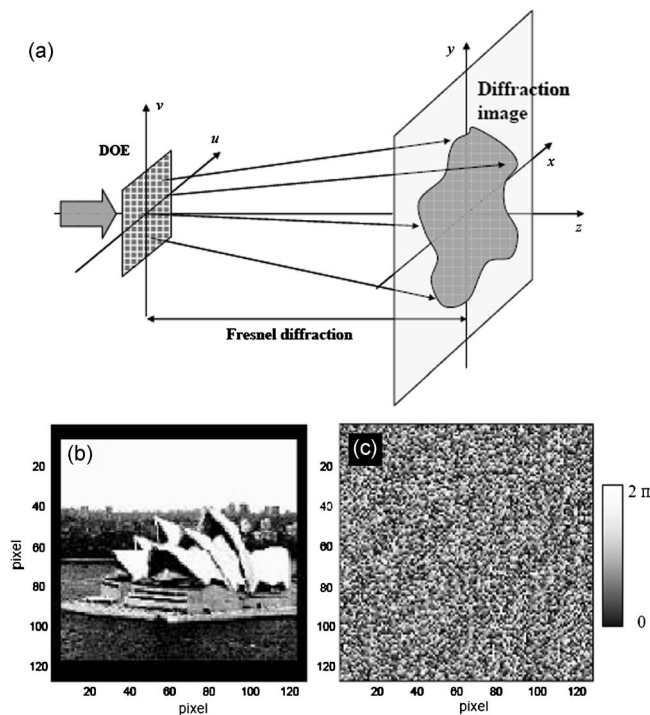


FIG. 1. (a) Incident beam is diffracted by a DOE with 128×128 pixels and forms a diffraction image in the output plane. (b) 2D intensity distribution of a photo of the Sydney Opera House sampled by 128×128 points. (c) Designed phase profile for (b) with 256 phase levels by using the iterative Fourier transform algorithm.

structure we fabricated was a polymer replica of this phase profile, as shown in Fig. 2(a). The sketch of the overall structure is a 3D surface structure with different heights in each pixel representing the phase information, which can be fabricated by the 2PP method in a polymer.

The material we employed for 2PP was a commercially available inorganic-organic hybrid polymer called Ormocer@s (Micro-Resist Technology). It shows low losses (high transparency) in both the visible and near-infrared wavelength regions, excellent thermal and mechanical properties, high chemical resistance, and low cost,⁸ which are highly desirable for the DOE fabrication.

Figure 2(b) depicts the optical setup for the DOE fabrication. A mode-locked Ti:sapphire laser (Mira 900F, Coherent) providing 140 fs pulses at a repetition rate of 76 MHz and an optical parametric oscillator (OPO) operating at 580 nm were employed to fabricate the DOE. The femtosecond pulses were focused by an oil-immersion microscope objective with a numerical aperture of 1.4. A charge coupled device camera was used to monitor the fabrication process in real time. The sample was mounted on a computer controlled piezoelectric scanning stage ($200 \times 200 \times 200 \mu\text{m}^3$, Physik Instrumente), which provided an arbitrary 3D motion of the sample. Because the operating wavelength of the OPO was well above the single-photon absorption wavelength of the resin, the laser beam can be focused into the volume of the resin without having any single-photon-induced polymerization reaction.

As can be seen from Fig. 2(c), each pixel of the fabricated DOE should be a cuboid with different heights. In our experiment, a lateral square crosssection of $1.56 \mu\text{m}$ was selected, which is determined by the maximum scanning range of the piezostage and the total number of pixels, as

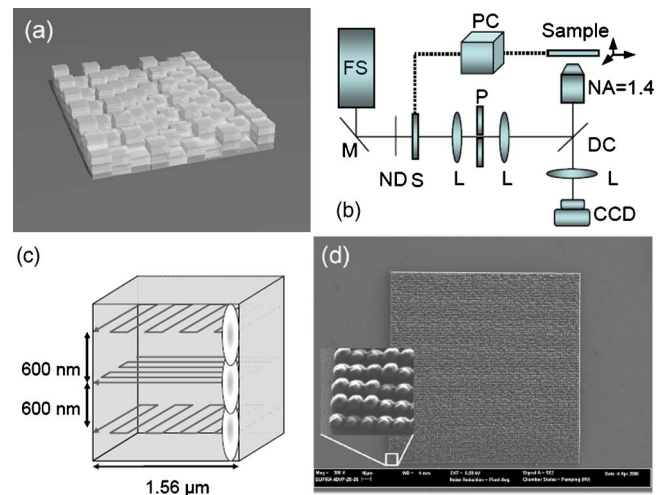


FIG. 2. (Color online) (a) Sketch showing an overall view of the designed DOE. The pixels are fabricated on a microscope cover glass. (b) Experimental setup for fabricating the DOE structures. FS: femtosecond laser combined with an OPO, M: mirror, ND: neutral density filter, S: shutter, L: lenses, P: pinhole, DC: dichroic mirror, and PC: computer for controlling the scanning stage and the shutter. (c) Scanning strategy for a single pixel. (d) SEM image of the fabricated DOE. The inset is a magnified corner of (d) indicated by a white square.

discussed later. The thickness t of a pixel corresponds to the phase modulation value of ϕ , given by

$$t = \frac{\lambda \phi}{2\pi(n_2 - n_1)}, \quad (3)$$

where n_1 and n_2 are the refractive indices of the ambient (i.e., air, $n_1 = 1$) and the DOE material (i.e., Ormocer, $n_2 = 1.5$). λ is the wavelength of the optical field. To generate a phase shift between 0 and 2π for a laser wavelength of 632.8 nm, one requires a pixel height varying between 0 and $1.5 \mu\text{m}$. For the used laser power of 1.6 mW the length of the polymerized voxel was approximately 700 nm. To fabricate pixels with a maximum height of $1.5 \mu\text{m}$, we had to scan the focal spot in three layers separated by 600 nm [see Fig. 2(c)]. The height of each pixel was defined by the position of the focal plane of the first layer relative to the glass substrate. The scanning pattern for each layer was a meander, as depicted in Fig. 2(c), and was rotated by 90° for each subsequent layer, which facilitates the generation of squarelike pixels. The scanning speed was $60 \mu\text{m/s}$, resulting in a total fabrication time of a couple of hours, which depends on the number of pixels in the designed phase profile.

To demonstrate the capability of continuous gray-level encoding, we produced two DOEs with 256 phase levels for generating a gray diffraction image and a binary diffraction image, respectively. Figure 2(d) presents a scanning electron microscope (SEM) image of one of the fabricated structures of an array of 128×128 pixels, in which a magnified image of a corner of the structure is also shown. It is clearly seen from the inset of Fig. 2(d) that pixels with different heights corresponding to 256 phase levels are well defined and the entire structure exhibits a high level of quality. Due to the spherical shape of the focal spot the fabricated pixels show a nonflat top surface rather than a flat one according to the design. However, the nonflat pixel surface does not affect the diffraction image because the high spatial-frequency shapes in a DOE pixel, resulting from sharp boundary edges between the adjacent pixels, do not significantly influence the

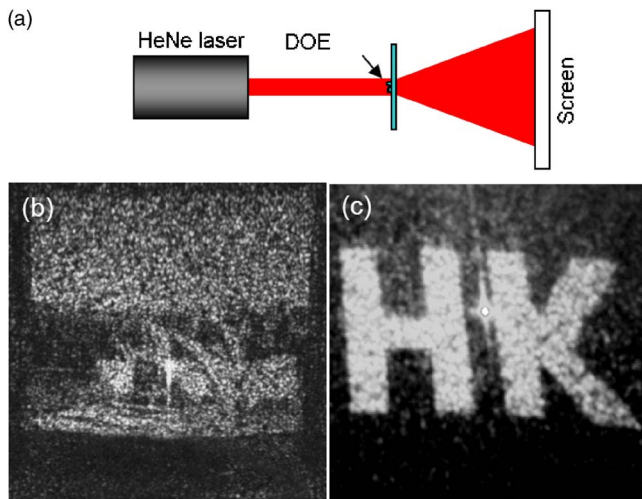


FIG. 3. (Color online) (a) Experimental setup for reconstructing the diffraction images from the DOEs fabricated by 2PP. (b) Reconstructed gray diffraction image of the Sydney Opera House. (c) Reconstructed binary diffraction image of the letters H and K.

far-field intensity distributions. On the contrary, the nonflat top pixel shape and the smooth boundary edges can reduce the optical power endowed to the higher-order diffraction images, which would be advantageous for some applications.

To characterize the fabricated DOEs, we irradiated the samples with a collimated He–Ne laser beam, as shown in Fig. 3(a). A screen was applied to collect the diffraction images. The reconstructed diffraction images of the Sydney Opera House and the binary letter image of letters H and K are presented in Figs. 3(b) and 3(c), respectively. One of the important quality factors of the DOE is the diffraction efficiency, defined as

$$DE = 100 \times \frac{\sum_{m,n \in S} |F_{m,n}|^2}{\sum_{m,n} |F_{m,n}|^2}, \quad (4)$$

where S denotes the signal area where the target intensity value $\bar{I}_{m,n}$ is defined. The measured diffraction efficiency of the binary letter image is 84%, which matches well with the theoretical estimation of 86.76% due to the accurate realization of the designed surface profile with high lateral resolution and 256 fine phase levels.

In our design, since the pixel size is set to $1.56 \mu\text{m}$, the image plane size given by $L_x = \lambda z / dx$ where λ , z , and dx are the wavelength, the distance between the DOE and the image plane, and the sampling interval, respectively, is 4.06 cm assuming that z is 10 cm. Thus, the image resolution ΔL_x defined as $\Delta L_x = \lambda z / N_x dx = \lambda z / H_x$, where N_x and H_x are the number of sampling and the DOE size, respectively, is

$316 \mu\text{m}$. It can be clearly seen that the image plane size is inversely proportional to the pixel size of the DOE and that the image resolution is directly proportional to the DOE size. Thus to increase the resolution of the resulting diffraction images, a larger dimension of the DOE is required. In practice, the large amount of “speckles” in a reconstructed image may be caused by the diffraction of the defects in the DOE, which result from the dislocation of the pixels during the fabrication of the DOE or during the postchemical processing.

In conclusion, we have proposed the use of the 2PP method to fabricate 3D DOEs encoded with continuous gray levels. The demonstrated multigray-level DOEs in the inorganic-organic hybrid polymer resin are not attainable with conventional semiconductor microlithography or arbitrarily complex surface relief techniques. A high diffraction efficiency of 84% approaching the theoretical limit has been achieved due to the high precision of the fabrication approach. This method is a mask-free and low-cost single-step fabrication process; therefore, it is promising for fabricating high quality DOEs encoded with phase information at any wavelength which is beyond the absorption of the used material.

This work was produced with the assistance of the Australian Research Council under the ARC Centres of Excellence program. The Centre for Ultrahigh-bandwidth Devices for Optical Systems (CUDOS) is an ARC Centre of Excellence. The authors thank Kyong Sik Choi for useful discussion.

¹J. Turunen and F. Wyrowski, *Diffraction Optics for Industrial and Commercial Applications* (Wiley, New York, 1997).

²V. A. Soifer, V. V. Kotlyar, and L. Doskolovich, *Iterative Methods for Diffraction Optical Elements Computation* (Taylor & Francis, London, 1997), Appendix G, pp. 219–229.

³C. Lee, Y. Chang, C. Wang, J. Chang, and G. Chi, *Opt. Lett.* **28**, 1260 (2003).

⁴J. Sohn, M. Lee, W. Kim, E. Cho, T. Kim, C. Yoon, N. Park, and Y. Park, *Appl. Opt.* **44**, 506 (2005).

⁵W. Daschner, M. Larsson, and S. H. Lee, *Appl. Opt.* **34**, 2534 (1995).

⁶W. Goltsos, S. Liu, and A. Sharlene, *Proc. SPIE* **1211**, 137 (1990).

⁷S. Kawata, H.-B. Sun, T. Tanaka, and K. Takada, *Nature (London)* **412**, 697 (2001).

⁸J. Serbin, A. Egbert, A. Ostendorf, B. N. Chichkov, R. Houbertz, G. Domann, J. Schulz, C. Cronauer, L. Frohlich, and M. Popall, *Opt. Lett.* **28**, 301 (2003).

⁹M. Straub and M. Gu, *Opt. Lett.* **27**, 1824 (2002).

¹⁰S. Wu, J. Serbin, and M. Gu, *J. Photochem. Photobiol., A* **181**, 1 (2006).

¹¹J. Serbin and M. Gu, *Adv. Mater. (Weinheim, Ger.)* **18**, 221 (2006).

¹²H. Kim, K. Choi, and B. Lee, *Jpn. J. Appl. Phys., Part 1* **45**, 6555 (2006).

¹³H. Kim, B. Yang, and B. Lee, *J. Opt. Soc. Am. A* **21**, 2353 (2004).

¹⁴H. Kim and B. Lee, *Jpn. J. Appl. Phys., Part 2* **43**, L702 (2004).